

Supplementary Materials for

Streptavidin-conjugated gold nanoclusters as ultrasensitive fluorescent sensors for early diagnosis of HIV infection

Aditya Dileep Kurdekar, L. A. Avinash Chunduri, C. Sai Manohar, Mohan Kumar Haleyurgirisetty, Indira K. Hewlett, Kamiseti Venkataramaniah*

*Corresponding author. Email: vrkamiseti@gmail.com

Published 21 November 2018, *Sci. Adv.* **4**, eaar6280 (2018)
DOI: 10.1126/sciadv.aar6280

This PDF file includes:

Fig. S1. HEX docking scores of the best poses for the increasing glutathione-NHS tails on the AuNC core with the streptavidin protein.

Fig. S2. TEM image of AuNCs, which indicates the size of the AuNCs to be around 2 nm or less.

Fig. S3. Absorption and emission spectra of AuNCs.

Fig. S4. Effect of the presence of interfering moieties on the GNCIA stability.

Fig. S5. Optimization of concentration of capture antibodies and AuNC-SA for optimal assay performance.

Table S1. Comparison of HEX energies of AuNC-SA for various capping agents on Au₁₃ cluster.

Table S2. Comparison of binding scores for gold, silver, and copper nanoclusters for increasing cluster sizes, where x denotes the number of atoms.

Table S3. Comparison of FP values of unconjugated AuNCs with conjugated AuNCs.

Table S4. Results of clinical serum analysis that shows the high specificity of GNCIA.

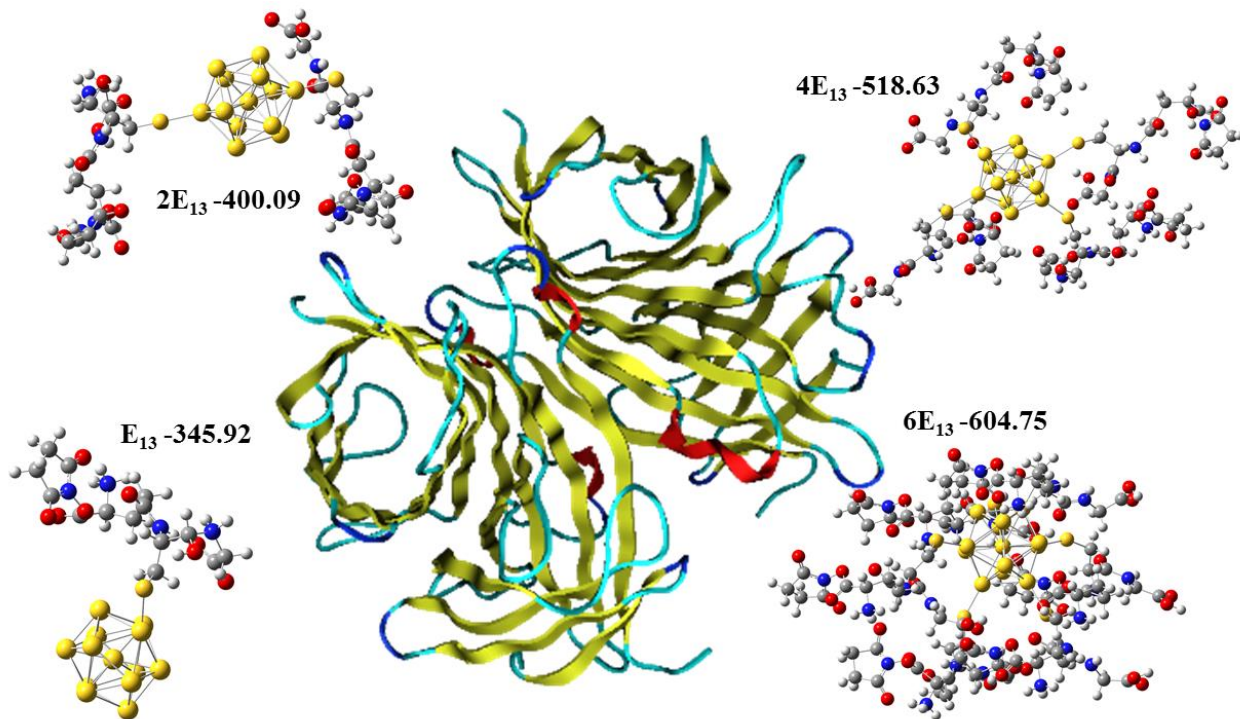


Fig. S1. HEX docking scores of the best poses for the increasing glutathione-NHS tails on the AuNC core with the streptavidin protein.

Morphological Characterization of Gold nanoclusters

The sample for TEM imaging was prepared by drop casting diluted solution of AuNCs on to a carbon coated copper grid and dried under vacuum before the analysis. The analysis of the TEM images of the gold nanoclusters was performed. Based on the size measurements of particles using ImageJ, the size of the clusters was confirmed to be 2 nm or less as seen in fig. S2. The particles were found to be monodispersed.

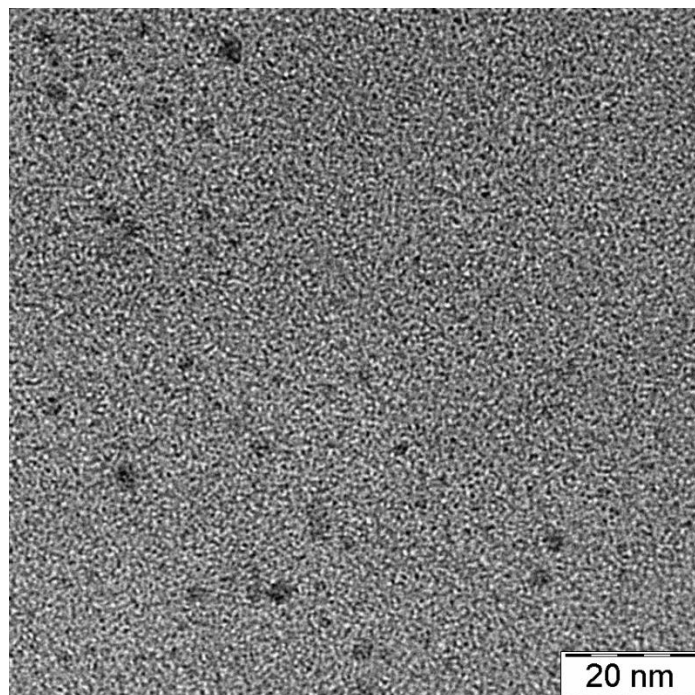


Fig. S2. TEM image of AuNCs, which indicates the size of the AuNCs to be around 2 nm or less.

UV-Visible absorption spectroscopy

Absorbance spectrum was obtained (Shimadzu UV-2450) by using UV-Vis absorption spectrophotometer. Figure S3 shows the UV-visible absorbance spectra of the glutathione capped AuNCs. The luminescent AuNCs have a unique UV-Vis absorption, which shows no characteristic peaks unlike the larger particles. A peak like feature observed at 400 nm can be attributed to UV absorption of conjugated glutathione as observed in many other nanoparticles(38). There was no surface plasma resonance (SPR at 520 nm is characteristic for spherical nanoparticles larger than 5 nm). This is indicative of their small size.

Photoluminescence Spectroscopy

Photoluminescence excitation and emission spectra were recorded on Spectramax M5 spectrophotometer. The gold nanoclusters exhibited broad emission at 615 nm when excited with 345 nm as shown in the fig. S3. The observed orange luminescence originates from the quantum confinement effects due to extra small size of these nanoclusters(39). The addition of glutathione also lead to creation of new states which resulted in the enhancement of fluorescence(40). Their

fluorescence remained unchanged for more than 3 months exhibiting their good colloidal stability which is highly needed for the immunoassay applications.

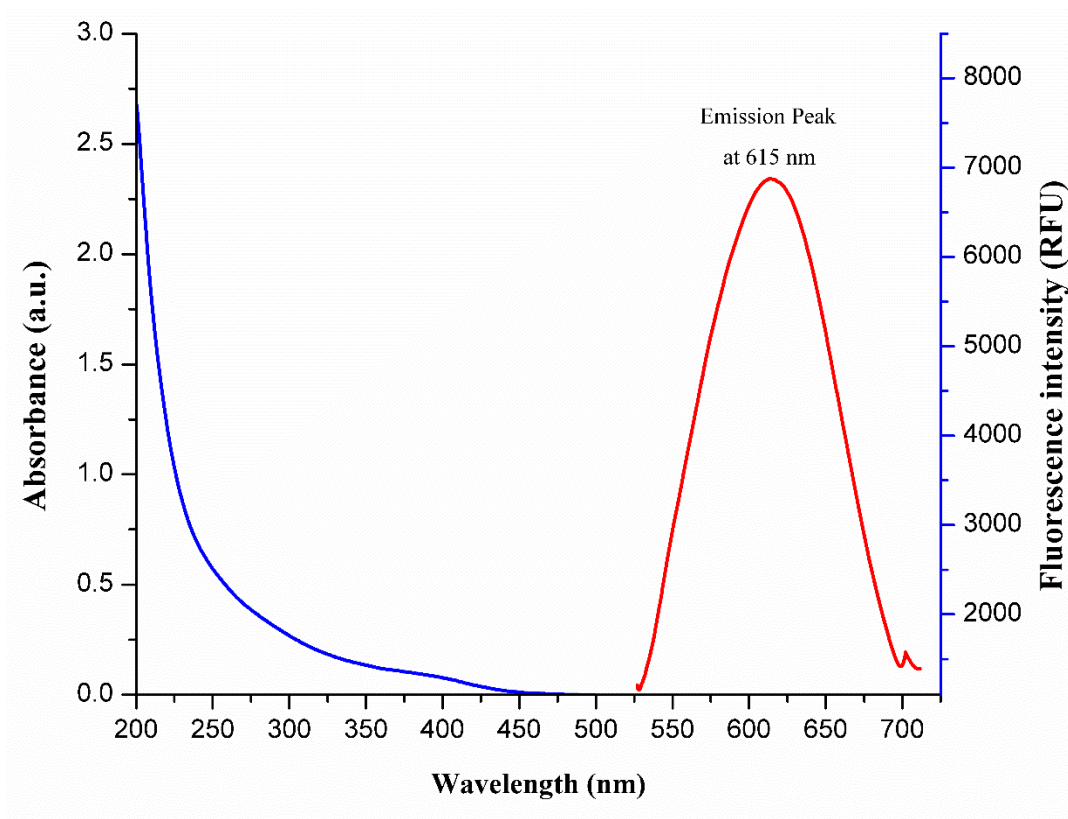


Fig. S3. Absorption and emission spectra of AuNCs. The shoulder peak nm is an absorption peak observed which when used as an excitation wavelength resulted in fluorescence emission at 615 nm

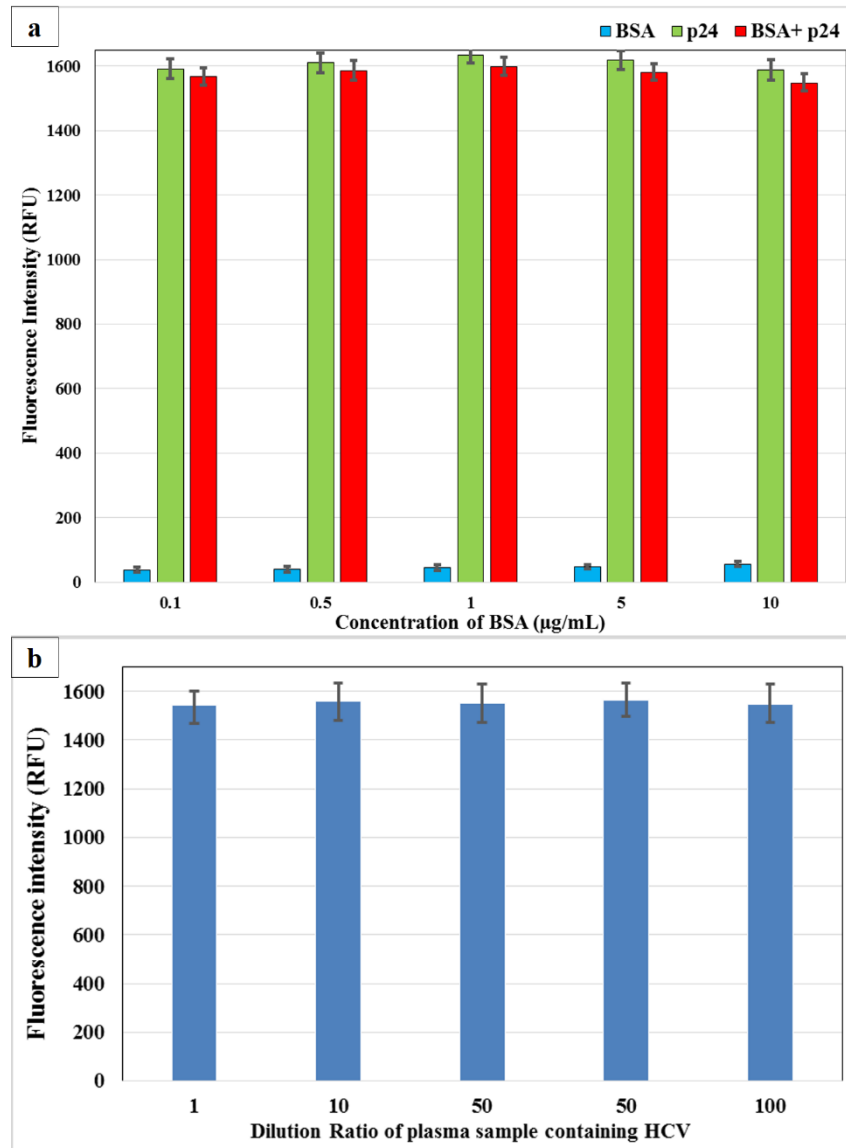


Fig. S4. Effect of the presence of interfering moieties on the GNCIA stability. (a) Plot of fluorescence intensities for 250 pg/mL p24 antigen in samples with varying concentration of BSA in comparison to the signal obtained from wells containing only BSA and only p24 antigen (b) Effect of dilution of HCV sample spiked with 250 pg/mL of p24 on fluorescence intensity from GNCIA. The clinical samples containing HCV were diluted to 5 different ratios. All the dilutions were spiked with the same quantity of HIV-1 p24 antigen. The graph plots the signal intensity for all 5 dilutions.

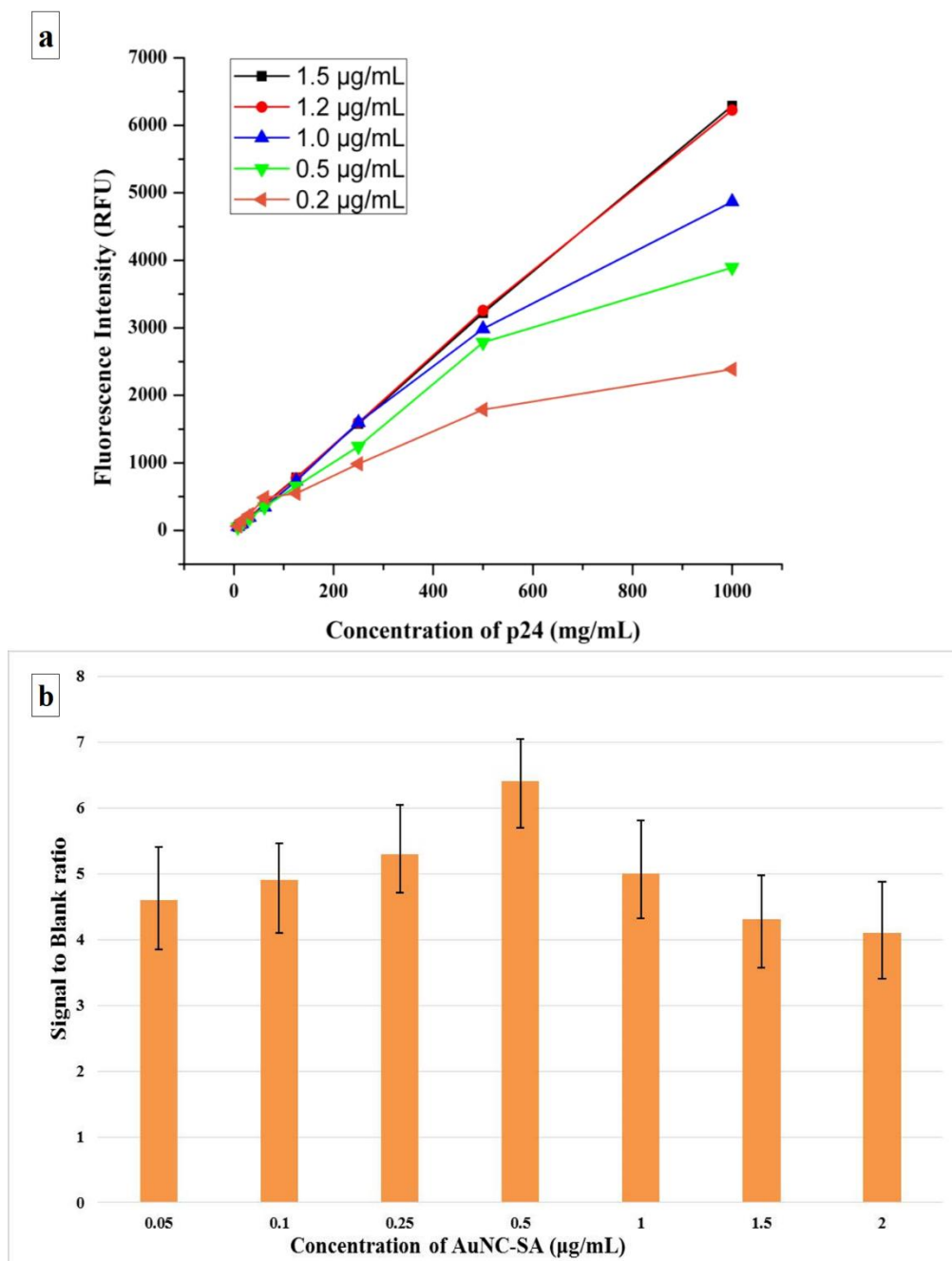


Fig. S5. Optimization of concentration of capture antibodies and AuNC-SA for optimal assay performance. (a) Effect of varying concentration of capture antibodies on fluorescence intensities in GNCA (b) Effect of varying concentration of AuNC-SA on signal to blank ratio in GNCA. The assay was performed with a fixed concentration of p24 of 250 pg/mL while varying the concentration of AuNC-SA in order to obtain the best signal to blank ratio²⁷.

Table S1. Comparison of HEX energies of AuNC-SA for various capping agents on Au₁₃ cluster.

S No.	Capping agent	Hex Energy
1	Glutathione	-513.19
2	11-mercaptoundecanoic acid	-508.66
3	L-3,4-dihydroxyphenylalanine	-457.14
4	D-penicillamine	-399.43
5	Mercapto-9-propyladenine	-488.51
6	N,N-dimethylformamide	-330.95

Table S2. Comparison of binding scores for gold, silver, and copper nanoclusters for increasing cluster sizes, where x denotes the number of atoms.

Metal nanoclusters	Binding score for Increasing cluster sizes				
	x=1	x=6	x=13	x=20	x=57
Ag _x	-41.87	-121.89	-147.85	-215.51	-332.71
Au _x	-42.25	-116.65	-137.72	-203.13	-318.67
Cu _x	-37.3	-114.95	-138.85	-185.36	-294.07

Table S3. Comparison of FP values of unconjugated AuNCs with conjugated AuNCs.

Sample	$I_{ }$	I_{\perp}	$FP = \frac{I_{ } - (G * I_{\perp})}{I_{ } + (G * I_{\perp})}$
Unconjugated AuNCs	95	78	0.098
Conjugated AuNCs	132	101	0.131

Table S4. Results of clinical serum analysis that shows the high specificity of GNCIA.

S. No	Sample type	No. of samples	No. of samples that tested positive for HIV	No. of Samples that tested negative for HIV
1	HIV positive	50	50	NIL
2	HIV negative	50	NIL	50
3	HIV negative/HBV positive	10	NIL	10
4	HIV negative/HCV positive	10	NIL	10